

CrossMark
click for updatesCite this: *J. Mater. Chem. C*, 2016,
4, 2925Received 23rd October 2015,
Accepted 1st December 2015

DOI: 10.1039/c5tc03480a

www.rsc.org/MaterialsC

Using membrane composition to fine-tune the pK_a of an optical liposome pH sensor†

Kasey J. Clear, Katelyn Virga, Lawrence Gray and Bradley D. Smith*

Liposomes containing membrane-anchored pH-sensitive optical probes are valuable sensors for monitoring pH in various biomedical samples. The sensitivity of the sensor is maximized when the probe pK_a is close to the expected sample pH. While some biomedical samples are close to neutral pH there are several circumstances where the pH is 1 or 2 units lower. Thus, there is a need to fine-tune the probe pK_a in a predictable way. This investigation examined two lipid-conjugated optical probes, each with appended deep-red cyanine dyes containing indoline nitrogen atoms that are protonated in acid. The presence of anionic phospholipids in the liposomes stabilized the protonated probes and increased the probe pK_a values by <1 unit. The results show that rational modification of the membrane composition is a general non-covalent way to fine-tune the pK_a of an optical liposome sensor for optimal pH sensing performance.

Introduction

In recent years there has been increased effort to develop optical sensors for measuring pH in a range of different biomedical samples.¹ In some cases, such the tumor micro-environment, the extracellular pH is in the weakly acidic range of 6.6–6.8, whereas in other disease states such as inflammation or infection, the pH can be as low as 5.5. To ensure the largest sensing dynamic range, it is helpful to fine-tune the sensor pK_a to match the pH of the sample under analysis.² If the sensor is a water-soluble dye, then an obvious approach is to synthetically modify the chemical structure, but this route often involves slow and resource intensive synthetic chemistry. An alternative approach is to covalently attach the dye to a polymeric scaffold and produce a pH sensing nanoparticle.^{3–6} In this case, the dye's acid-sensitive equilibrium can be modulated by additional attachment of charged groups,⁷ but a limitation with this approach is the need to conduct additional synthetic chemistry on the polymer backbone.

A simpler synthetic strategy is to anchor the dye in self-assembled nanoparticles and non-covalently incorporate charged components to control the dye pK_a . Possible choices for the nanoparticles are biocompatible micelles or liposomes.^{8,9} There is a body of literature showing how micelle composition can be used to control dye pK_a ,^{10–12} but micelles are not sufficiently stable

to serve as robust sensors for certain applications. In the case of liposomes, there are scattered reports on the effect of membrane composition on anchored pH-responsive molecules,^{13–15} but there seems to be no systematic studies on the magnitude of the effect. Furthermore, most of these studies have focused on the fluorescent response, and in many cases the results are hard to interpret due to medium-induced changes in the fluorescence quantum yield.^{16–18} With a long-term plan to develop optical sensors for pH measurements in various biomedical samples, we chose to investigate two lipid-anchored conjugates of pH-responsive pentamethine cyanine (Cy5) dyes (Scheme 1). The dyes are fluorescent compounds, and their deep red absorption/emission bands are well-suited for biological imaging. Our goal was to measure the pK_a change induced by anchoring the dye in a liposome membrane and also by changing the membrane composition. The results allow us to describe a set of general guiding principles for systematic fine-tune control of the pK_a of optical probes within a liposome sensor.

Experimental

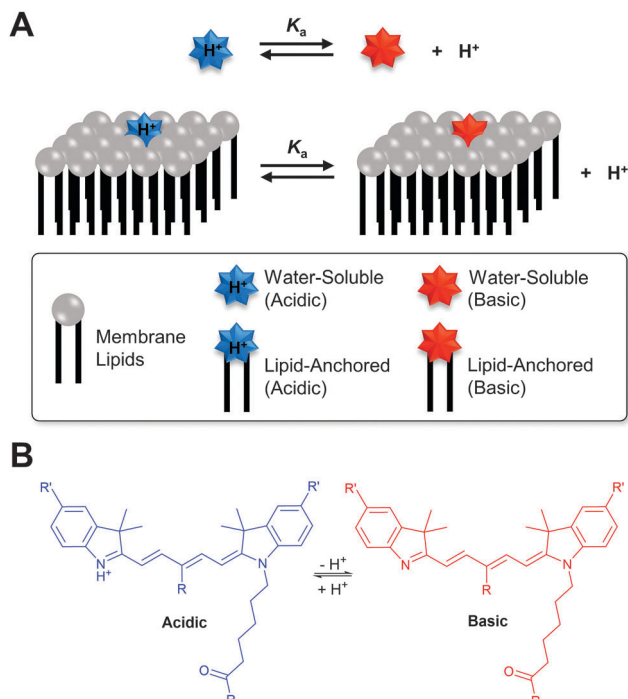
Materials and chemical analysis

Unless indicated otherwise, organic reagents and solvents were used as provided by Sigma-Aldrich. POPA, POPC, POPG, and POPS‡ were purchased from Avanti Polar Lipids and stored in $CHCl_3$ at $-20\text{ }^\circ\text{C}$. NMR solvents were obtained from Cambridge

Department of Chemistry and Biochemistry, University of Notre Dame,
236 Nieuwland Science Hall, Notre Dame, Indiana 46556, USA.
E-mail: smith.115@nd.edu

† Electronic supplementary information (ESI) available: Lipid structures, pH titration absorbance spectra, fluorescence titration curves, synthesis, and characterization data. See DOI: 10.1039/c5tc03480a

‡ Abbreviations: POPA, 1-palmitoyl-2-oleoyl-*sn*-glycero-3-phosphate, sodium salt; POPC, 1-palmitoyl-2-oleoyl-*sn*-glycero-3-phosphocholine; POPG, 1-palmitoyl-2-oleoyl-*sn*-glycero-3-phosphoglycerol, sodium salt; POPS, 1-palmitoyl-2-oleoyl-*sn*-glycero-3-phosphoserine, sodium salt.



Scheme 1 (A) Cartoon representation of the protonation of water-soluble and lipid-anchored pH-sensitive probes. (B) Structure of acidic and basic forms of pH-responsive dyes.

Isotope Labs and NMR spectra were acquired at room temperature on either a Varian DirectDrive 600 MHz spectrometer or a Bruker AVANCE III HD 500 MHz spectrometer. Chemical shifts are reported in ppm and spectra were referenced to the residual solvent signal. In the case of solvent mixtures, the NMR spectra were referenced to the major solvent component. LC-MS was performed using a Dionex RSLC coupled to a Bruker micrOTOF Q II with a Dionex Acclaim RSLC 120 C18 2.2 μm 2.1 \times 100 mm reversed-phase column. Mobile phase A = water with 0.1 formic acid; mobile phase B = acetonitrile with 0.1% formic acid. Flow rate = 0.4 mL min^{-1} and column temp = 50 degrees. The initial mobile phase was 95% A/5% B which was ramped to 100% B. The LC eluent entered the electrospray source of the micrOTOF Q II and was analyzed by the Q-TOF mass analyzer. Full synthetic details can be found in the ESI.†

Continuous buffer preparation

To facilitate the preparation of buffers of different pH and for consistency between the buffer in the liposome studies, experiments with Cy5 probes 2 and 4 used a continuous buffer composed of a ternary mixture of borate, citrate, and phosphate (4 : 1 : 2 molar ratio) reported previously.¹⁹ The buffer was prepared at 10 mM concentration of the ternary mixture with 137 mM NaCl and 3.2 mM KCl and the pH was adjusted by the addition of aqueous HCl or NaOH (1 M or 6 M solutions).

Liposome preparation

The appropriate molar amounts of lipids and probe 2 or 4 (2 mol%) in chloroform solutions were mixed in a clean test tube,

and the solvent was evaporated under a stream of argon and the lipid film was placed under high vacuum at room temperature for more than one hour. The lipid film was hydrated by addition of continuous buffer at pH 7 to give a stock solution with total lipid concentration of 5 mM that was vortexed at room temperature for 2 minutes. The dispersion of multilamellar liposomes was extruded 21 times through a nucleopore polycarbonate membrane (0.2 μm) to give a stock solution of unilamellar liposomes incorporating either probe 2 or 4.

pK_a determination

Continuous buffer (10 mM) at a range of pH values was added to wells of a 96-well microtiter plate suitable for bottom-read fluorescence measurements (Greiner Bio One). Liposome stock solution with incorporated probe was added to give a final concentration of 100 μM in each well with three replicates for each pH value. The microtiter plate was agitated for 5 minutes and then left to incubate at room temperature for 2–3 hours to ensure complete equilibration of pH between the liposome interior and outside solution. The absorbance and fluorescence spectra were measured at 22 $^\circ\text{C}$ using a SpectraMax M5 microplate reader. The absorbance ratio of $A_{\text{acid}}/A_{\text{base}}$ was plotted as a function of pH for each liposome composition. This data was converted to pK_a using the sigmoidal curve fitting function in GraphPad software.

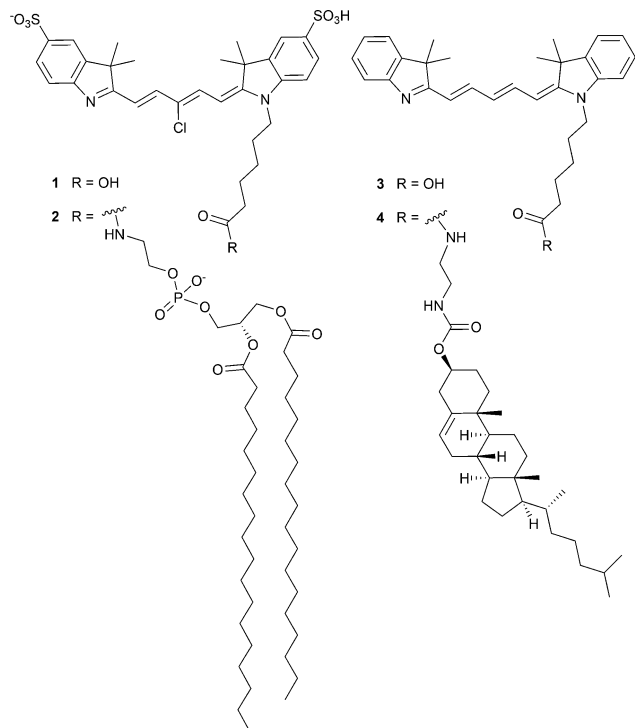
Results and discussion

Synthesis and properties of pH-responsive dyes and lipid-conjugate probes

The pH-responsive dye 1 (Scheme 2), with an appended carboxylic acid, was prepared by a literature method²⁰ and subsequently coupled to the phospholipid 1,2-distearoyl-*sn*-glycero-3-phosphoethanolamine (DSPE) by amide bond formation to give the highly amphiphilic phospholipid conjugate 2. Dye 3, a more lipophilic version of 1, was synthesized by a similar procedure, and then converted into the cholesterol conjugate 4 by amide bond coupling with an amine functionalized cholesterol derivative.²¹

The dyes and lipid-conjugate probes are deep-red fluorescent compounds and their absorbance and emission maxima are summarized in Table 1. While the fluorescence properties are more likely to be utilized for pH sensing applications, we have focused this pK_a study on changes in absorbance spectra, thereby eliminating any experimental artifacts associated with fluorescence efficiency. But the reader should note that all dye and probe titrations were monitored by changes in absorption and fluorescence. The fluorescence data is provided in the ESI† and replicates the trends exhibited by the following absorption data.

Comparison of dye 1 in aqueous solution and its DSPE-conjugate probe 2 anchored in liposomes composed of zwitterionic POPC‡ reveals an 11 nm bathochromic shift in absorbance of the protonated (acidic) form in liposomes. This is consistent with the red shift observed when cyanine dyes are measured in organic solvents compared to aqueous buffer, and suggests that



Scheme 2 Structures of pH-responsive dyes, **1** and **3**, and the corresponding lipid-conjugate probes, **2** and **4**.

Table 1 Properties of probes **2** and **4** in POPC liposomes and corresponding free dyes **1** and **3** in buffer

Probe	Absorption λ_{max} (nm), acidic	Absorption λ_{max} (nm), basic	Emission λ_{max} (nm)	pK_{a}
Dye 1 ^a	646	506	663	6.29 ± 0.04
Probe 2 ^b	655	480	672	5.15 ± 0.02
Dye 3 ^a	638	490	659	6.98 ± 0.07
Probe 4 ^b	648	478	670	5.44 ± 0.02

^a 1 μM dye in 10 mM continuous buffer. ^b 100 μM POPC liposomes containing 2 mol% probe in continuous buffer at 22 °C.

the dye component in probe **2** embeds into the membrane interfacial region.²² A similar red shift effect (10 nm) is apparent when the absorption maxima for the acidic form of dye **3** in water is compared to the corresponding band for cholesterol-linked probe **4** incorporated into POPC liposomes.

The pK_{a} values for the two dyes (**1** and **3**) in buffer solution and the two probes (**2** and **4**) in liposomes were determined by conducting absorption titration experiments. For the liposome systems, the pH responsive probes were incorporated at 2 mol% loading into the lipid film prior to liposome hydration and extrusion. The probe pK_{a} was calculated by first equilibrating separate samples of liposomes in different pH solutions and acquiring the absorbance spectrum. Fig. 1 shows representative titration spectra for probes **2** and **4** in liposomes, highlighting the shift from cyan absorbance at high pH to red absorbance at low pH, with an isosbestic point between the absorption bands (see Fig. S2 and S3 for full set of titration spectra, ESI†).

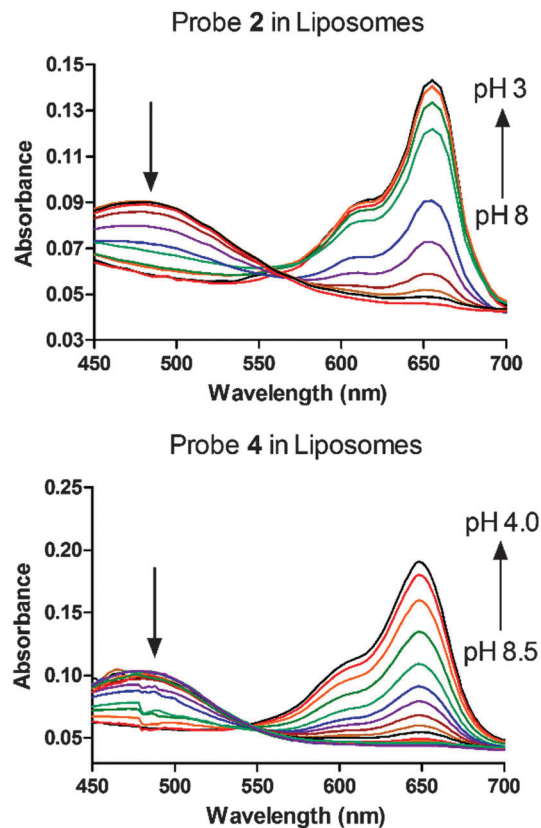


Fig. 1 Representative absorption spectra for probes **2** and **4** in liposomes composed of 10:90 POPS:POPC (2 mol% added probe) as a function of pH. Total lipid concentration was 100 μM , and the buffer was composed of 10 mM continuous buffer (see Experimental), with 137 mM NaCl and 3.2 mM KCl at 22 °C.

The ratio of absorption values, $A_{\text{acidic}}/A_{\text{basic}}$, for the protonated and unprotonated maxima bands was plotted as a function of pH, and the sigmoidal plots were fitted by nonlinear methods to obtain probe pK_{a} values.

Inspection of Table 1 shows that the pK_{a} of the dye component in the membrane-embedded probe was more than 1 unit lower than the free dye in aqueous buffer. A change in the apparent pK_{a} for a pH-sensitive molecule as it is moved from bulk water to a membrane surface is expected.^{18,23} For example, a similar pK_{a} decrease was observed in a pH-sensitive rhodamine lipid conjugate,²⁴ but the opposite trend (pK_{a} increase) was seen with a fluorescein²⁵ and a seminaphthorhodafluor (SNARF) conjugate.²⁴ A reconciling explanation for these seemingly inconsistent results is the decreased polarity of the membrane interface favoring the less polar structure in each of these pH-sensitive equilibria. In the case of nitrogen-based Cy5 and rhodamine dyes, the less polar structure is the deprotonated (basic) form, but in the case of fluorescein and SNARF dyes the less polar structure is the protonated (acidic) form.

It is not surprising that the dye component in lipophilic probe **4** is buried in the membrane, but perhaps a little unexpected that the more polar dye component in probe **2** with its charged functional groups also partitions into the membrane. However, this behavior agrees with literature reports showing that charged dyes covalently linked to membrane anchors can penetrate into

shallow membrane depths.^{26,27} A comparison of the pK_a changes for each dye/probe pair shows that ΔpK_a is 1.1 for probe 2 and 1.6 for probe 4, which suggests that the more lipophilic dye component in 4 is buried more deeply in the bilayer membrane.

Effect of phospholipid composition on probe pK_a

In Fig. 2A and B are plots of the absorbance ratios for each probe, 2 and 4, in liposomes containing different fractions of anionic POPS, and in Fig. 2C is a plot of probe pK_a values as a function of the mol% of POPS.‡ In both cases, the probe pK_a increased by >0.5 units as the mol% of POPS was raised from

Table 2 pK_a values of probes 2 and 4 in liposomal membranes

Probe	POPC	10% POPS	20% POPS	35% POPS	50% POPS
2	5.15 ± 0.02	5.23 ± 0.01	5.39 ± 0.02	—	5.78 ± 0.02
4	5.44 ± 0.02	5.54 ± 0.01	5.74 ± 0.01	5.95 ± 0.02	6.31 ± 0.02

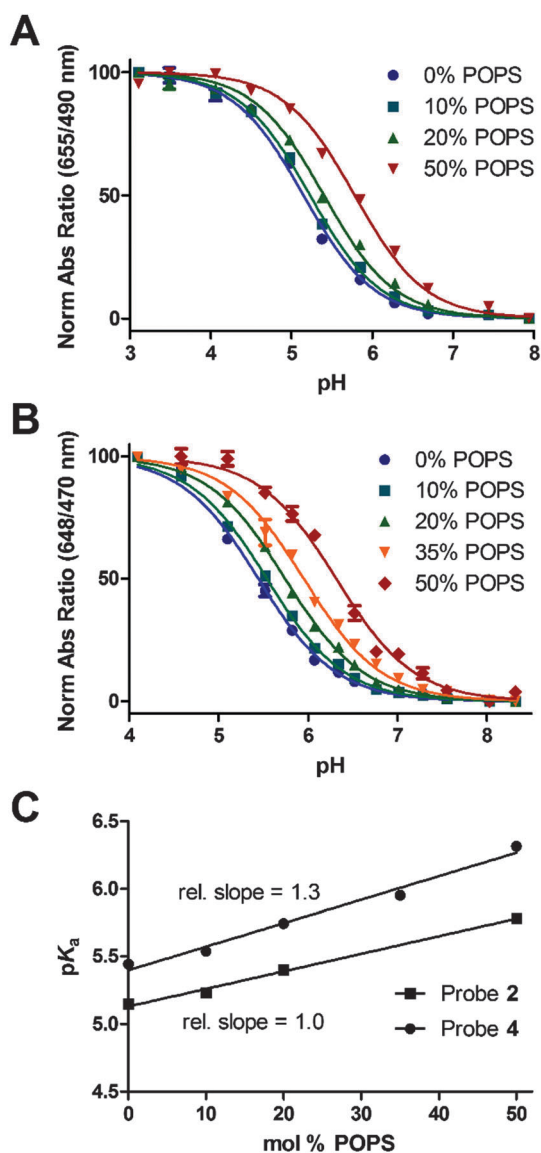


Fig. 2 pH titration curves for probes 2 (A) and 4 (B) in liposomes composed of varying mole ratios of POPS:POPC (2 mol% added probe). The normalized absorbance ratio (A_{acidic}/A_{basic}) is plotted as a function of pH, along with the sigmoidal curve fitting for each data set. Total lipid concentration was 100 μ M, and the buffer was composed of 10 mM continuous buffer, with 137 mM NaCl and 3.2 mM KCl. Each titration point is the mean and standard deviation of three ratio measurements at each pH value. (C) Computed pK_a as a function of mol% POPS for probes 2 and 4.

zero to 50% (Table 2). The slopes in Fig. 2C indicate that the more lipophilic probe 4 is more sensitive to changes in POPS levels than probe 2. This agrees with the model of different partitioning depth for the dye component on the two probes. The more lipophilic dye in probe 2 is partitioned deeper into the membrane and thus is more strongly affected by the presence of added POPS. This conclusion is supported by a previous literature study which compared the response of a set of pH-sensitive probes to increasing proportions of charged lipids.¹⁵ In this literature work, the authors found that the sensitivity to charged additives in the membrane decreased when the probe's dye component partitioned at shallower depths in the membrane.

In principle, the change in probe pK_a caused by the added POPS could be due to direct non-covalent interaction of the probe with the POPS head-group, or alternatively a nonspecific membrane surface electrostatic effect. There is literature evidence for both types of effects. For example, it is known that divalent cation and peripheral protein binding events can alter the microenvironment at a membrane interface and thus affect the apparent pK_a of membrane bound lipids and dyes.^{28–30} Conversely, the interfacial electrostatic surface potential has been observed to drive changes in pK_a for optical probes in micelles,³¹ pH responsive spin labels in liposomes,^{13,32} and liposome insertion rates by transmembrane peptides.³³ To distinguish these possible explanations, the pH titration experiments were repeated using liposomes containing probe 2 and 20 mol% of POPS or the analogous anionic phospholipids, POPA, and POPG.‡ As shown in Fig. 3, the titration profile of probes 2 and 4 did not change with the identity of the anionic phospholipid in the liposomes, strongly suggesting that the charge of the membrane constituents was more important than the structure of the phospholipid head group.

From a practical perspective these results nicely show how the same pH sensitive membrane-anchored probe can be fine-tuned for optimal pK_a in different imaging and pH sensing applications. For example, the pK_a value for membrane-anchored probe 4 in POPC liposomes is 5.44, a value that is well-suited for imaging studies that detect liposome uptake into endosomes that can reach the acidic pH range of 5.0–5.5.§ But this pK_a value is too

‡ While the main goal of this study was to ascertain the sensitivity of probe pK_a values to membrane composition, it is worth summarizing the expected capabilities of liposome anchored probes 2 and 4 as fluorescent pH sensors. The fluorescent properties for each probe are listed Table S1 (ESI[†]) and they are in the normal range for deep-red Cy5 dyes. They are photostable to repeated scanning in a fluorometer, but like all Cy5 dyes they likely will undergo some bleaching in a more intense microscopy experiment that produces reactive oxygen species. However, an advantage of ratiometric molecular probes like 2 and 4 is that any probe bleaching should not alter the ratiometric response. The probe response to changes in pH is reversible and the response time is controlled by the diffusion of protons across the liposome membrane, which is typically complete within a few minutes, but can be accelerated by the presence of very small amounts of lipophilic ion transporters in the liposome membrane.²⁴

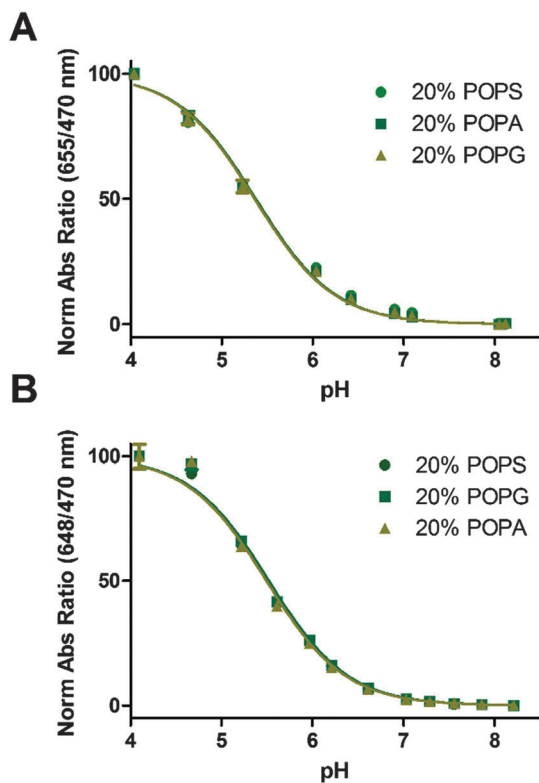


Fig. 3 The influence of anionic phospholipid structure on titration curves for probe 2 (A) or probe 4 (B) (2 mol%) in liposome membranes comprised of POPC with 20 mol% of POPS, POPA, or POPG. Graphed is the normalized absorbance ratio ($A_{\text{acidic}}/A_{\text{basic}}$) as a function of pH with a plot of sigmoidal curve fitting for each data set.

low for accurate imaging studies of the tumor extracellular pH, which is typically in the range of 6.6–6.8. In this latter case, a much better choice of liposome composition is POPC:POPS (1 : 1) where the pK_a for membrane-anchored probe 4 is 6.31. Indeed, we recently demonstrated a specific example of this sort of pK_a optimization in the area of photoacoustic imaging. We altered the composition of liposomes containing a lipophilic near-infrared pH-sensitive dye and maximized the change in ratiometric photoacoustic signal produced when the liposomes were in the acidic peritoneal cavity of a living mouse.³⁴ While the two liposome sensors in this present study use anionic membrane additives to raise the probe pK_a values, there is no doubt that cationic additives would produce the reverse trend. But in the case of membrane-anchored probes 2 and 4 this would lower the pK_a values to <5, which does not have much biological relevance.

Conclusions

The pK_a of liposome-anchored optical probes can be modulated in a systematic way by including charged amphiphiles in the liposome membrane. This investigation examined two lipid-conjugate optical probes, each with appended deep-red cyanine dyes containing indoline nitrogen atoms that are protonated in acid. The presence of anionic phospholipids in the liposomes stabilized the protonated probes and increased the probe

pK_a values. More specifically, changing the liposome membrane composition from 100% zwitterionic POPC to anionic POPC:POPS (1 : 1) raised the pK_a of the two liposome-anchored optical probes by 0.6 and 0.9, respectively. The results indicate that systematic variation of the membrane composition is a general non-covalent way to fine-tune the pK_a of an optical liposome pH sensor by <1 unit so that it can better match the sample pH and achieve a higher sensing sensitivity.

Acknowledgements

This work was supported by the NIH (GM059078), a GAANN fellowship, and the University of Notre Dame.

Notes and references

- 1 D. Wencel, T. Abel and C. McDonagh, *Anal. Chem.*, 2014, **86**, 15–29.
- 2 R. V. Benjaminsen, H. Sun, J. R. Henriksen, N. M. Christensen, K. Almdal and T. L. Andresen, *ACS Nano*, 2011, **5**, 5864–5873.
- 3 P. Kumar E. K, L. N. Feldborg, K. Almdal and T. L. Andresen, *Chem. Mater.*, 2013, **25**, 1496–1501.
- 4 Y. Bao, H. De Keersmaecker, S. Corneillie, F. Yu, H. Mizuno, G. Zhang, J. Hofkens, B. Mendrek, A. Kowalczyk and M. Smet, *Chem. Mater.*, 2015, **27**, 3450–3455.
- 5 X.-d. Wang, J. A. Stolwijk, T. Lang, M. Sperber, R. J. Meier, J. Wegener and O. S. Wolfbeis, *J. Am. Chem. Soc.*, 2012, **134**, 17011–17014.
- 6 R. V. Søndergaard, J. R. Henriksen and T. L. Andresen, *Nat. Protoc.*, 2014, **9**, 2841–2858.
- 7 H. Sun, T. L. Andresen, R. V. Benjaminsen and K. Almdal, *J. Biomed. Nanotechnol.*, 2009, **5**, 676–682.
- 8 Q. Liu and B. J. Boyd, *Analyst*, 2013, **138**, 391–409.
- 9 M. Horie, H. Yanagisawa and M. Sugawara, *Anal. Biochem.*, 2007, **369**, 192–201.
- 10 M. E. D. Garcia and A. Sanz-Medel, *Talanta*, 1986, **33**, 255–264.
- 11 N. O. McHedlov-Petrosyan, N. A. Vodolazkaya, A. G. Yakubovskaya, A. V. Grigorovich, V. I. Alekseeva and L. P. Savvina, *J. Phys. Org. Chem.*, 2007, **20**, 332–344.
- 12 P. Fromherz, in *Methods Enzymol.*, ed. B. F. Sidney Fleischer-Academic Press, 1989, vol. 171, pp. 376–387.
- 13 M. A. Voinov, I. Rivera-Rivera and A. I. Smirnov, *Biophys. J.*, 2013, **104**, 106–116.
- 14 G. Duportail, A. Klymchenko, Y. Mely and A. Demchenko, *FEBS Lett.*, 2001, **508**, 196–200.
- 15 R. Kraayenhof, G. J. Sterk and H. W. Wong Fong Sang, *Biochemistry*, 1993, **32**, 10057–10066.
- 16 C. J. MacNevin, D. Gremyachinskiy, C.-W. Hsu, L. Li, M. Rougie, T. T. Davis and K. M. Hahn, *Bioconjugate Chem.*, 2013, **24**, 215–223.
- 17 A. Toutchkine, V. Kraynov and K. Hahn, *J. Am. Chem. Soc.*, 2003, **125**, 4132–4145.
- 18 X.-X. Zhang, Z. Wang, X. Yue, Y. Ma, D. O. Kiesewetter and X. Chen, *Mol. Pharmaceutics*, 2013, **10**, 1910–1917.
- 19 W. R. Carmody, *J. Chem. Educ.*, 1961, **38**, 559–560.

- 20 S. A. Hilderbrand, K. A. Kelly, M. Niedre and R. Weissleder, *Bioconjugate Chem.*, 2008, **19**, 1635–1639.
- 21 M. Avadisian, S. Fletcher, B. Liu, W. Zhao, P. Yue, D. Badali, W. Xu, A. D. Schimmer, J. Turkson, C. C. Gradinaru and P. T. Gunning, *Angew. Chem., Int. Ed.*, 2011, **50**, 6248–6253.
- 22 D. S. Pisoni, L. Todeschini, A. C. A. Borges, C. L. Petzhold, F. S. Rodembusch and L. F. Campo, *J. Org. Chem.*, 2014, **79**, 5511–5520.
- 23 M. S. Fernandez and P. Fromherz, *J. Phys. Chem.*, 1977, **81**, 1755–1761.
- 24 G. C. Kemmer, S. A. Bogh, M. Urban, M. G. Palmgren, T. Vosch, J. Schiller and T. G. Pomorski, *Analyst*, 2015, **140**, 6313–6320.
- 25 C. G. Knight and T. Stephens, *Biochem. J.*, 1989, **258**, 683–687.
- 26 E. Asuncion-Punzalan, K. Kachel and E. London, *Biochemistry*, 1998, **37**, 4603–4611.
- 27 K. Kachel, E. Asuncion-Punzalan and E. London, *Biochim. Biophys. Acta*, 1998, **1374**, 63–76.
- 28 J. J. Shin and C. J. Loewen, *BMC Biol.*, 2011, **9**, 85.
- 29 W. Wang, N. A. Anderson, A. Travasset and D. Vaknin, *J. Phys. Chem. B*, 2012, **116**, 7213–7220.
- 30 H. Jung, A. D. Robison and P. S. Cremer, *J. Am. Chem. Soc.*, 2009, **131**, 1006–1014.
- 31 G. V. Hartland, F. Grieser and L. R. White, *J. Chem. Soc., Faraday Trans. 1*, 1987, **83**, 591–613.
- 32 M. A. Voinov, I. A. Kirilyuk and A. I. Smirnov, *J. Phys. Chem. B*, 2009, **113**, 3453–3460.
- 33 A. Kyrychenko, V. Vasquez-Montes, M. B. Ulmschneider and A. S. Ladokhin, *Biophys. J.*, 2015, **108**, 791–794.
- 34 S. Guha, G. Shaw, T. Mitcham, R. R. Bouchard and B. D. Smith, *Chem. Commun.*, 2016, DOI: 10.1039/C5CC08317F.